# TWO PORT RECONFIGURABLE CIRCULAR PATCH ANTENNA FOR MIMO SYSTEMS

**D. Piazza*†, P. Mookiah*, M. D'Amico† and K.R. Dandekar***

* Electrical & Computer Eng. Dept., Drexel Univ., Philadelphia, PA 19104, USA.
dp84@drexel.edu, pm352@drexel.edu, dandekar@ece.drexel.edu
† Electrical & Computer Eng. Dept., Politecnico di Milano., Milano,20133, Italy.
damico@elet.polimi.it

**Keywords:** reconfigurable antennas, MIMO, smart antennas, adaptive communications.

## Abstract

In this paper we demonstrate a novel reconfigurable multi-port circular patch antenna that improves the performance of a MIMO wireless communications system through pattern diversity. Different modes of the circular patch antenna can be excited by varying its radius with PIN diode switches. The performance achievable with such reconfigurable antennas in a 2x2 MIMO communication system is evaluated using computational electromagnetic ray tracing simulations and channel measurements in an indoor environment. The results show an improvement in throughput while reducing the physical size of the antenna array on the communication device.

## Introduction

The requirements for next generation air interfaces seek to provide reliability and high data rate at low cost. Multiple Input Multiple Output (MIMO) antenna systems have emerged as one of the most significant technical breakthroughs in modern wireless communications able to satisfy these stringent requirements [1]. However the necessity of assuring a high data rate in a large variety of environments while reducing antenna array space occupation on portable devices requires an improvement in current MIMO technology.

Recent studies have shown that employing reconfigurable antennas can improve the gains offered by a Multiple Input Multiple Output (MIMO) system [2, 3]. These antennas adaptively change their electrical and radiation properties according to the propagation characteristics of the wireless channel in order to provide a "strong" channel between the transmitting and receiving antennas, in a given communication system.

In this paper we propose a two port reconfigurable circular patch antenna (RCPA) that can be varied in radius through PIN diode switches. The antenna exploits the principle of pattern diversity in order to provide: (i) increased data rate compared to common non reconfigurable antennas, (ii) reduced space occupation by the antenna on the communication device and (iii) a reduced number of radio-frequency chains needed at the receiver/transmitter.

The performance of the proposed antenna is studied, in terms of channel Shannon capacity, in a 2x2 802.11n MIMO system employing a spatial multiplexing transmission scheme. The benefits derived from using the proposed reconfigurable MIMO antenna system are determined and compared with non-reconfigurable antenna systems using both computational electromagnetic simulation and experimental field-testing in an indoor environment.

## 2 Reconfigurable Circular Patch Antenna (RCPA)

In this section we present a compact two port reconfigurable circular patch antenna (RCPA) intended to be used as a building block of a 802.11n MIMO communication system. The antenna design uses a single physical antenna with two feed points that allows a two-element array to be realized within a small footprint on the communication device.

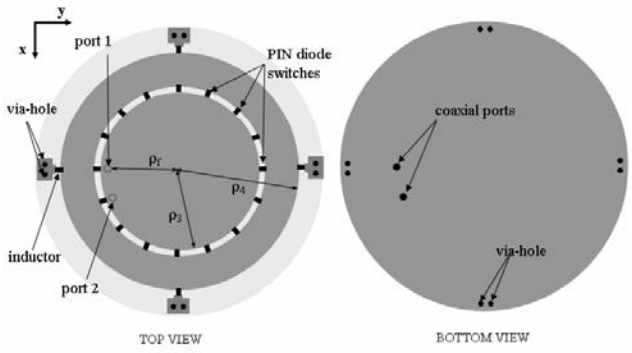


Figure 1: RCPA antenna design (top and bottom view).

### A. Antenna Structure

The RCPA, first introduced by the authors in [4], consists of a circular patch with two accessible coaxial ports that is capable of reconfiguring its radiation pattern at each port. Two different radiation patterns can be excited at each port varying opportunely the current distribution over the patch. A detailed schematic of the RCPA is shown in Figure 1.

In order to change the current distribution on the antenna, the radius of the circular patch is varied. By varying the patch size, different electromagnetic modes of circular patch

antenna can be excited and each excited mode generates a unique radiation pattern in the far-field [5].

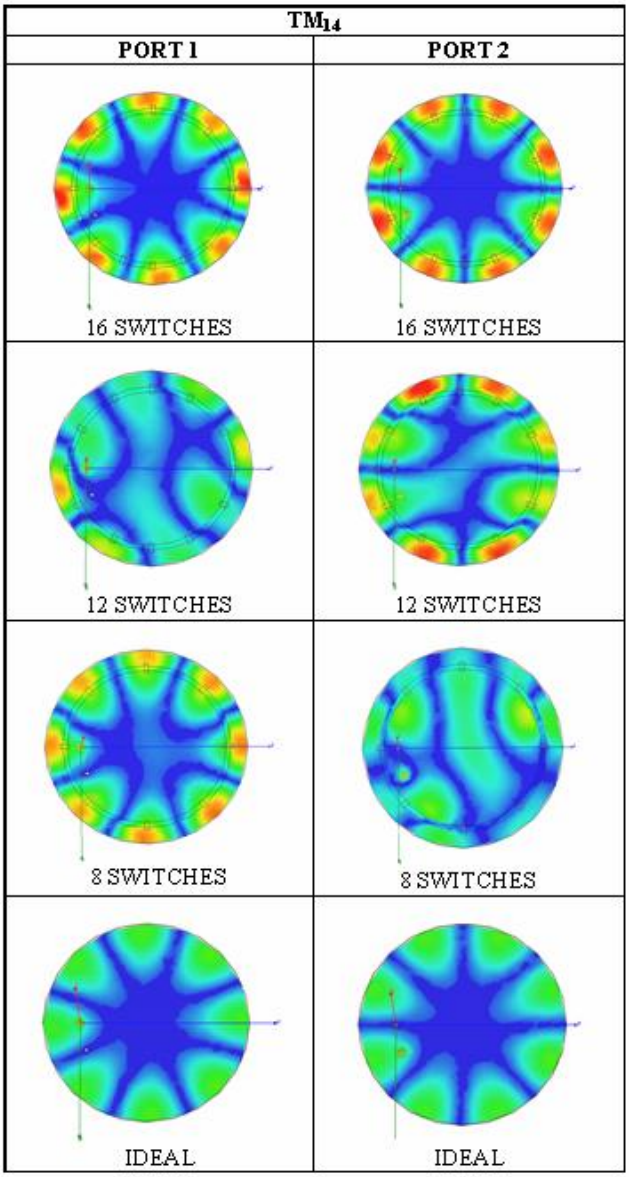


Figure 2: Electric field distribution in the antenna substrate for "mode 4" configuration as a function of the number of switches.

The antenna is built on FR4 substrate and the radius of the circular patch is varied using PIN diodes switches strategically located over the antenna structure. Two different configurations of the antenna can then be defined at each port: one in which all the switches are turned off and the electromagnetic mode $TM_{13}$ is excited ("mode 3") and another in which they are turned on and the electromagnetic mode $TM_{14}$ is excited ("mode 4").
As investigated through electromagnetic simulations in the finite difference time domain (FDTD) a minimum of sixteen switches are necessary in order to properly excite the electromagnetic mode $TM_{14}$ at both the antenna ports. As depicted in Figure 2 the electric field in the antenna substrate, and therefore the current on the circular patch, is not distributed in the characteristic way of mode $TM_{14}$ when less than sixteen switches are placed on the antenna structure. Note also that the switches need to be placed where the electric field is maximum for mode $TM_{14}$. PIN diode switches with an isolation of 18 dB and an insertion loss of 0.3 dB at a frequency of 2.5 GHz are used and placed in parallel to one another allowing for reduced power losses.
Four pads symmetrically located around the circular patch, are used to provide a ground for the biasing current of the PIN diodes. 1000 nH inductors are used to isolate the radio frequency signal from the DC ground. The DC bias (current of 10 mA and voltage of 0.7 V) is directly provided from one of the two feed points through a wideband coaxial bias-tee.
The two ports on the antenna structure are separated by 25° such that they are well isolated and the radiation patterns excited simultaneously at the two ports are spatially orthogonal to each other. The distance of the two ports from the center of the patch is strategically selected in order to have both ports matched at a frequency of 2.484 GHz for both antenna configurations.
In Table 1 a summary of the structural parameters for the antenna is provided.

| ANTENNA STRUCTURAL PARAMTERS | |
|---|---|
| Dielectric | FR4 ($\varepsilon_r = 4.4$) |
| Number of switches | 16 |
| Feeds separation | 25° |
| Dielectric thickness | 0.1524 mm |
| $\rho_f$ | 3.82 cm |
| $\rho_3$ | 3.9 cm |
| $\rho_4$ | 4.6 cm |

Table 1: List of structural parameters of the RCPA.

### *B.* Scattering Parameters

The scattering parameters of the antenna structure have been measured with a network analyzer and simulated using the finite-difference time-domain method HFSS antenna design software.
Figure 3 and Figure 4 show the measured and simulated scattering parameters of the RCPA determined at the two input ports over frequency, and for both antenna configurations ("mode 3" and "mode 4"). For both configurations, there is an isolation of about 20 dB and the return loss is below the target -10 dB at any port in the band of interest. The large isolation between the two ports allows for the generation of orthogonal radiation patterns, using a single antenna structure as a two element array. The -10 dB bandwidth of the RCPA is 1%, denoting the narrow-band characteristic of the proposed antenna.

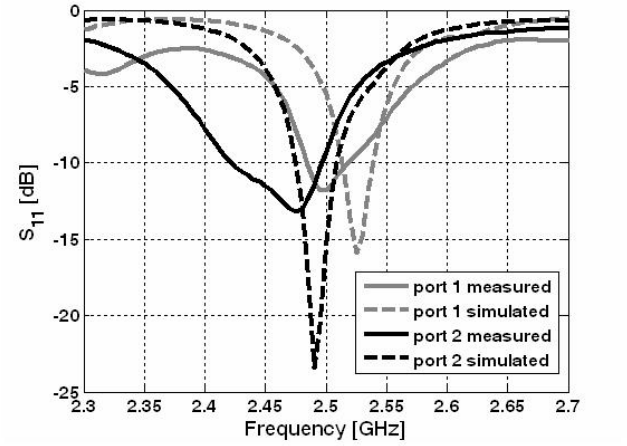


(a)

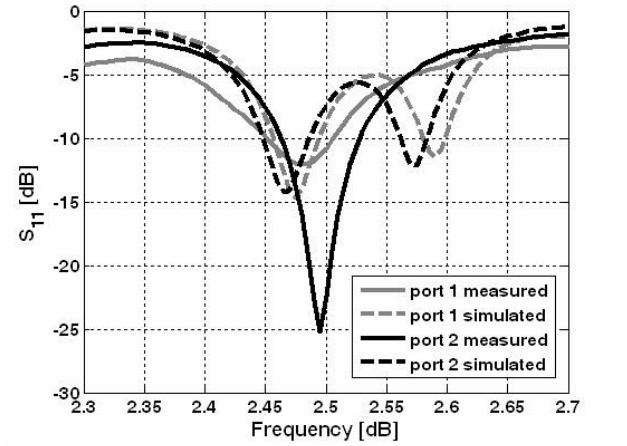


(b)

Figure 3: Measured and simulated reflection coefficient at the two ports of the RCPA for (a) "mode 3" configuration and (b) "mode 4" configuration.

### *C.* Radiation Characteristics

The radiation properties of the RCPA have been simulated using HFSS antenna design software. Figure 5 shows the simulated electric field radiation patterns of the two configurations of the RCPA in the azimuthal and elevation (φ = 0°) plane at a frequency of 2.484 GHz. The diversity between the radiation patterns of different configurations is also of interest. The main differences can be observed in the azimuthal plane where the radiation pattern of "mode 3" has six main beams compared to the eight of the "mode 4" configuration. As discovered in Section 2A, note also that the radiation patterns excited at the two ports are orthogonal to one another: where there is a maximum in radiation at port 1, there is a null in radiation at port 2. Looking at the radiation pattern in the elevation plane we can also notice that the "mode 3" configuration has a maximum at 46° while "mode 4" has a maximum at 56°. The maximum directivity is 7 dB for "mode3" and 9 dB for "mode4".

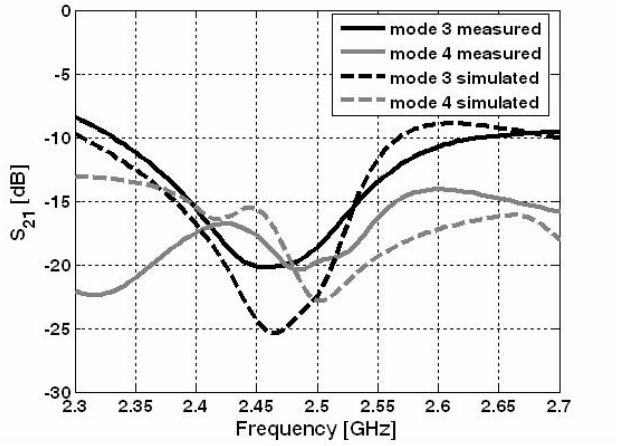


Figure 4: The simulated isolation between the two ports of the RCPA for both the antenna configurations ("mode3" and "mode4").

The level of diversity between the patterns generated at the two ports of the RCPA, as well as between the patterns generated at the same port for different configurations of the array, is estimated through the spatial correlation coefficient value [6, 7]. Assuming a rich scattered environment, the spatial correlation coefficient, $\rho_{j,k,l,m}$ ,is defined as [7]:

$$\rho_{j,k,l,m} = \frac{\int_{4\pi} E_{j,k}(\Omega) E_{l,m}^{\dagger}(\Omega) d\Omega}{\left[\int_{4\pi} \left|E_{j,k}(\Omega)\right|^2 d\Omega \int_{4\pi} \left|E_{j,k}(\Omega)\right|^2 d\Omega\right]^{1/2}} \quad (1)$$

where $j$ and $l$ define the array port and $k$ and $m$ the antenna configuration at the port $j$ and $l$ respectively. $E_{j,k}(\Omega)$ is the radiation pattern of the configuration $k$ at port $j$ over the solid angle $\Omega = (\phi, \theta)$ and † denotes the complex conjugate transpose operator. Table 2 shows the values of correlation between patterns generated at the two ports of the antenna, while Table 3 shows the values of correlation between patterns generated at the same port for all the array configurations. It can be noted from Table 2 that the correlation values between radiation patterns at the two ports of the RCPA are almost zero and therefore small enough ($\rho_{j,k,l,m} \leq 0.7$) for all the configurations to provide significant diversity gain [6]. Also from Table 3, it can be observed that the patterns generated at the same port for different configurations are orthogonal to one another allowing for maximum pattern diversity.

| | $E_{1,\text{mode3}}$ | $E_{1,\text{mode4}}$ |
|---|---|---|
| $E_{2,\text{mode3}}$ | 0.01 | N/A |
| $E_{2,\text{mode4}}$ | N/A | 0.04 |

Table 2: Spatial correlation values between radiation patterns generated at the two ports of the RCPA.

| | $E_{1,mode3}$ | $E_{1,mode4}$ |
|---|---|---|
| $E_{1,mode3}$ | 1 | 0.07 |
| $E_{1,mode4}$ | 0.05 | 1 |

Table 3: Spatial correlation values between radiation patterns generated at the same port of the RCPA.

## 3 System Model

The proposed antenna is specifically designed to be used in MIMO communication systems. In particular in this work we analyze the benefit deriving from applying the RCPA in a MIMO system that employs a spatial multiplexing transmission scheme in order to improve the signal to noise ratio (SNR) at the receive antennas.

We assume a flat fading channel that is unknown at the transmitter. $\mathbf{H}_{j,k} \in C^{N_r \times N_t}$ is the transfer channel matrix of a MIMO system with $N_t$ transmit antennas in the $j$-th configuration and $N_r$ receive antennas in the $k$-th configuration. The signal collected at the receiver is related to the signal outgoing from the transmitter through the relation:

$$\mathbf{y} = \mathbf{H}\mathbf{x} + \mathbf{n} \qquad (2)$$

where $\mathbf{y}_{j,k} \in C^{N_r \times 1}$ is the signal vector at the receiver array, $\mathbf{x}_{j,k} \in C^{N_t \times 1}$ is the signal vector at the transmit antenna array and $\mathbf{n}_{j,k} \in C^{N_r \times 1}$ is the complex additive white Gaussian noise (AWGN) vector.

The channel capacity of such communication system is defined as [8]:

$$C = \log_2 \left[ \det \left( \mathbf{I}_{N_r} + \frac{SNR}{N_t} \mathbf{H}_{j,k} \mathbf{H}_{j,k}^{\dagger} \right) \right] \qquad (3)$$

where $\mathbf{I}_{N_r}$ is a $N_r \times N_r$ identity matrix, $\dagger$ denotes a complex conjugate transpose operation, and $SNR$ is the average signal-to-noise-ratio over all receiver array elements.

## 4 Simulations and Measurements

The performance that can be achieved, in terms of channel capacity, using the proposed RCPA in a 2x2 MIMO communication system employing a spatial multiplexing transmission scheme was investigated through electromagnetic ray tracing simulations and channel measurements in an indoor environment.

A total of six communication links were considered as depicted in Figure 6. The transmitter was static while the receiver was moved to six different locations. Both line of sight (LOS) and non line of sight (NLOS) links were considered

The RCPA was employed both at the receiver and the transmitter of the communication link; therefore a total of four different antenna configurations were offered per communication link (two at the transmitter and two at the receiver).

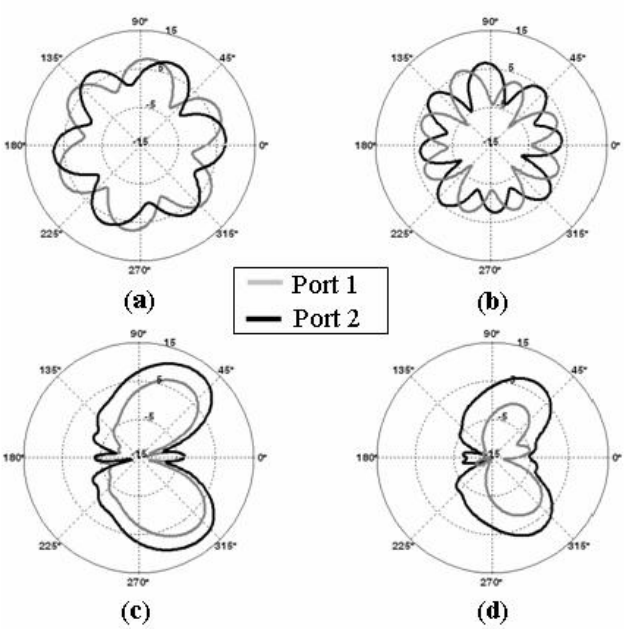


Figure 5: Simulated radiation patterns (in dB) of the RCPA both in the azimuthal ((a) and (b)) and elevation ((c) and (d)) plane at the frequency of 2.484 GHz. The radiation patterns are reported for the two antenna ports and for both the RCPA configurations: (a) and (c) "mode 3", (b) and (d) "mode 4".

### *A.* Simulation Setup

The channel capacity was determined via numerical computation using an electromagnetic ray tracer, FASANT [9]. FASANT is a deterministic ray tracing program based on geometric optics and the uniform theory of diffraction. A 3D model of the hallway of the 3rd floor of the Bossone Research building on Drexel University campus was simulated as the geometry input of FASANT.

Both the transmitting and receiving nodes were located at a height of 1.5 m. For each receiver location, the node was moved on a 10x10 grid of points (100 points) separated 0.03 $\lambda$ in order to perform local averaging and simulate the small scaling effects of the wireless channel.

The simulated 3D radiation patterns of the RCPA were used in the ray tracing simulation both at the receiver and at the transmitter in a 2x2 MIMO system. Note that the orientation of the reconfigurable antennas was selected such that the maximum degree of pattern diversity between the different antenna configurations was in the azimuthal plane.

As a means of comparison, the channel capacity was also determined for 2x2 MIMO systems employing half wavelength dipoles with a half wavelength (lambda/2) and one wavelength (lambda) spacing.

The simulations were conducted by transmitting a single tone at 2.484 GHz to obtain the values of the entries of the channel matrices, **H**, for each communication link.

### *B.* Measurement Setup

The channel capacity achievable using the proposed RCPA was measured with a 2x2 MIMO Orthogonal Frequency Division Multiplexing (OFDM) testbed communication system.

Each node of the experimental platform consisted of frequency agile transceivers operating in the ISM and UNII radio bands and a baseband process computer. The baseband chassis had two major functional roles. First, the unit contained the analog to digital (A/D) and (D/A) converters required for the two transceivers. The converters operated at 100 MS/s with 14-bit quantization. Second, the baseband unit was a software defined radio (SDR) which allowed the physical layer to be flexible in implementing different experiments.

The measurements were taken in the same indoor environment used for simulations. The measurements were performed at 2.484 GHz. We used BPSK to generate the analog baseband signal. The analog signal obtained was modulated using OFDM with the data being sent on each of the 52 sub-carriers. The spacing between each sub carrier was 312.5 kHz. A training pattern using binary phase shift keying (BPSK) was transmitted independently over the two transmitters. This training pattern was then received and used to estimate the channel matrix, **H**, for each communication link.

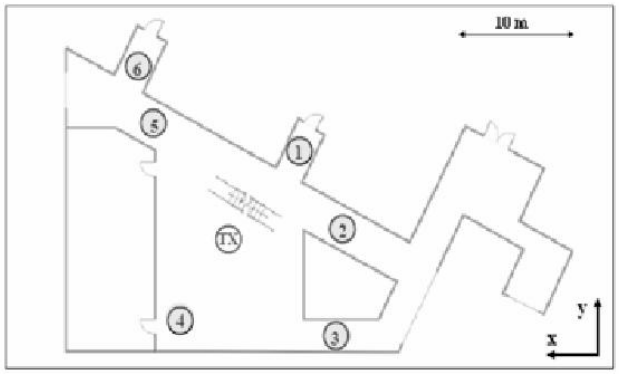


Figure 6: Indoor environment model. The transmitter and the receiver locations are indicated.

### *C.* Channel Capacity

The channel capacity of each 2x2 MIMO communication link is calculated according to equation (3). In order to remove the difference in path loss among a number of channel matrices, a Frobenius normalization of the channel matrix was computed [10]. Specifically, to preserve the relative antenna gain effects of each configuration, all the channel matrices for each receiver location were normalized with respect to the "mode 3" channel matrix. The normalization factor is defined as:

$$NF = \sqrt{\frac{\left\| \mathbf{H}_{"mode3-mode3"} \right\|_F^2}{N_t N_r}} \qquad (4)$$

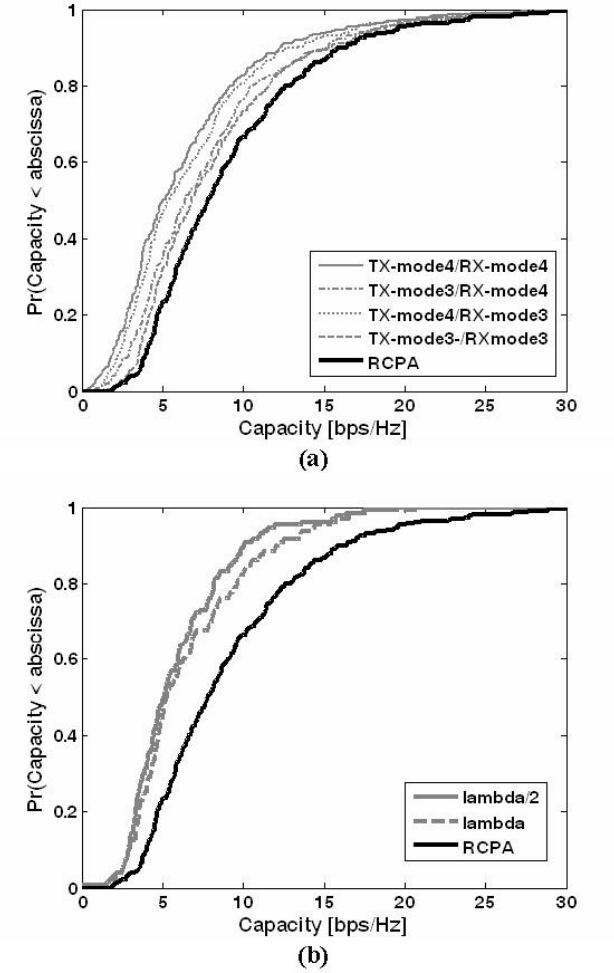


Figure 7: CDF of the simulated channel capacity for the RCPA and (a) for the four different configurations of the RCPA in a link and (b) for half wavelength dipoles spaced λ and λ/2. SNR=10 dB.

## 5 Results

Based on the data collected from simulations, a cumulative distribution function (CDF) for the channel capacity using the RCPA was numerically computed and reported in Figure 7 for a SNR = 10 dB. In Figure 7(a) one curve represents the CDF of channel capacity for the RCPA, while the other curves are relative to the channel capacity of each of the four possible configurations of the RCPA used individually in a link. The results show an achievable gain of 1.2 bps/Hz with respect to a system employing circular patch antennas in

"mode 3" for an outage probability of 50 %. The gain is even higher (2.8 bps/Hz) if we compare the RCPA with a system employing circular patch antennas in "mode 4". In Figure 7(b) the channel capacity achievable with the RCPA is compared with 2x2 MIMO systems employing half wavelength dipoles spaced a half wavelength (lambda/2) and one wavelength (lambda) apart. The RCPA achieves a capacity gain of 2.4 bps/Hz and 2.8 bps/Hz with respect to half wavelength dipoles spaced lambda and lambda/2 respectively, while occupying less space on the communication device.

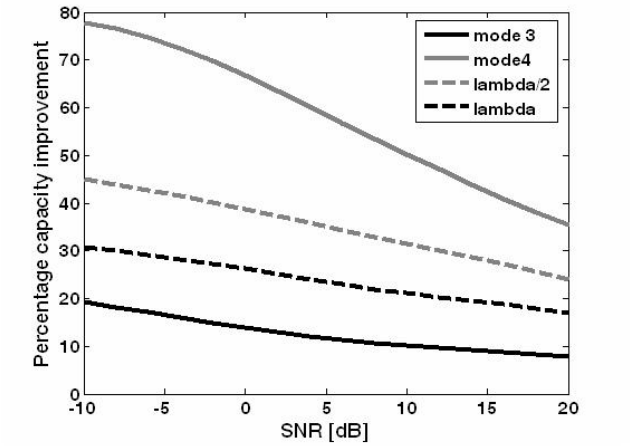


Figure 8: Simulated percentage average capacity improvement achievable with the RCPA in function of the SNR at the receiver. The improvement is calculated with respect to a system employing over the communication link circular patches in "mode3", circular patches in "mode4" and half wavelength dipoles spaced lambda and lambda/2.

In Figure 8 we show the average percentage of channel capacity improvement, as a function of the SNR at the receiver, achievable with the proposed RCPA with respect to a system that employs circular patch antennas operating in "mode 3" and in "mode 4" and half wavelength dipoles spaced lambda and lambda/2. The average capacity improvement varies as a function of the SNR at the receiver. The proposed antenna solution guarantees higher gain when the SNR is lower at the receiver. For a SNR of -5 dB the percentage improvement is about 17% and 75% with respect to non-reconfigurable two-port circular patches operating in "mode 3" and "mode 4" respectively, while for a SNR of 20 dB the improvement drops down to 9% and 35% respectively. In the same way, the gain achievable with respect to half wavelength dipoles spaced lambda and lambda/2 is 29% and 43% for a SNR of -5 dB and 18% and 24% for a SNR of 20 dB respectively.

In Figure 9 , we show the cumulative distribution functions of the channel capacity obtained from measurements for the RCPA and for non reconfigurable circular patch operating in "mode 3" and "mode 4", for a SNR of 10 dB. It can be noted that the measurement data confirm the results generated through simulations. The results show an achievable capacity improvement, with 50% probability, of 15% and 52% with respect to a system employing circular patch antennas in "mode 3" and "mode 4" respectively.

In Figure 10, we show the percentage average capacity improvement achievable with the proposed RCPA with respect to a non reconfigurable circular patch antenna operating in "mode 3", as a function of the SNR at the receiver. The percentage average capacity improvement is shown for each of the six locations occupied by the receiver in the indoor environment. It can be noted that the improvement achievable with the proposed reconfigurable antenna varies as a function of the antenna location and therefore as a function of the multipath environment. For three of the six locations, the RCPA outperforms a conventional non reconfigurable antenna operating in "mode 3", while for the other three locations the antenna configuration that guarantees the highest channel capacity is "mode 3". Also note that, in accordance with the results of Figure 8, the average capacity improvement is higher for low SNR values at the receiver. Averaging the capacity improvement over the six different locations, we find the capacity gain offered by the RCPA is about 14% for a SNR of 20 dB and 25% for a SNR of 0 dB.

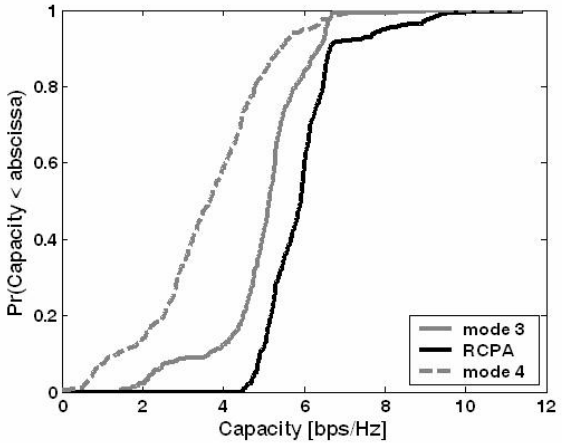


Figure 9: CDF of the measured channel capacity for the RCPA and for circular patch antennas operating in "mode 3" and "mode 4". SNR=10 dB.

## 6 Conclusions

A novel reconfigurable antenna that can be used as a building block of a reconfigurable MIMO transceiver has been proposed. Measurements and simulation results have shown that this antenna, exploiting the principle of pattern diversity, is capable of providing higher channel capacity and a more reliable communication link with respect to conventional non reconfigurable antenna systems. The compact design of the antenna allows also for reduced space occupation by the antenna on the communication device.

Future work will involve developing novel reconfigurable antennas that have more degrees of reconfigurability and that

can combine the benefit of pattern and polarization diversity in order to improve the achievable capacity gain.

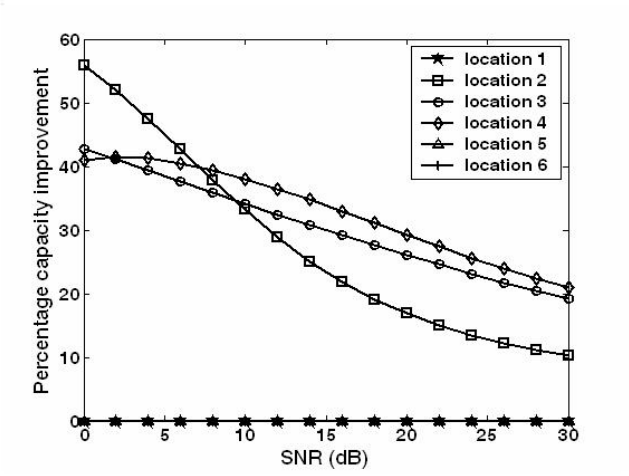


Figure 10: Measured percentage average capacity improvement achievable with the RCPA in function of the SNR for different receiver locations. The improvement is calculated with respect to a system employing over the communication link circular patches in "mode3".

## Acknowledgements

The authors would like to thank Mr. Nicholas Kirsch for his help in conducting the field measurements described in this paper. This material is based upon work supported by the U.S. National Science Foundation under grants 0435041 and 0322795. National Instruments has provided equipment donations supporting this research.

## References

[1] G. J. Foschini and M. J. Gans, "On limits of wireless communications in a fading environment when using multiple antennas," *Wireless Personal Communications,* vol. 6, pp. 311-335, 1998.

[2] D. Piazza and K. R. Dandekar, "Reconfigurable antenna solution for MIMO-OFDM systems," *Electronics Letters,* vol. 42, pp. 15-16, 2006.

[3] B. A. Cetiner, H. Jafarkhani, J.-Y. Qian, H. J. Yoo, A. Grau, and F. De Flaviis, "Multifunctional reconfigurable MEMS integrated antennas for adaptive MIMO systems," *IEEE Communications Magazine,* vol. 42, pp. 62-70, 2004.

[4] D. Piazza, P. Mookiah, M. D'Amico, and K. Dandekar, "Computational electromagnetic analysis of a reconfigurable multiport circular patch antenna for MIMO communications," *to appear in Proceedings of the International Symposium on Electromagnetic Theory, EMTS,* 2007.

[5] R. G. Vaughan, "Two-port higher mode circular microstrip antennas," *IEEE Transactions on Antennas and Propagation,* vol. 36, p. 3, 1988.

[6] C. Waldschmidt, J. V. Hagen, and W. Wiesbeck, "Influence and modelling of mutual coupling in MIMO and diversity systems," in *IEEE Antennas and Propagation Society, AP-S International Symposium (Digest)*, 2002, pp. 190-193.

[7] R. G. Vaughan and J. B. Andersen, "Antenna diversity in mobile communications," *IEEE Transactions on Vehicular Technology,* vol. T-36, pp. 149-172, 1987.

[8] M. Jankiraman, *Space time codes and MIMO systems*: Artech House, 2004.

[9] M. F. Catedra, J. Perez, A. Gonzalez, O. Gutierrez, and F. Saez de Adana, "Fast computer tool for the analysis of propagation in urban cells," *Annual Wireless Communications Conference, Proceedings, ,* pp. 240-245, 1997.

[10] M. A. Jensen and J. W. Wallace, "A review of antennas and propagation for MIMO wireless communications," *IEEE Transactions on Antennas and Propagation,* vol. 52, pp. 2810-2824, 2004.